GEOPHYSICS, VOL. 85, NO. 5 (SEPTEMBER-OCTOBER 2020); P. Q11–Q26, 7 FIGS., 3 TABLES.
10.1190/GEO-2019-0674.1

Comparison of monotonicity challenges encountered by the inverse scattering series and the Marchenko demultiple method for elastic waves

C. Reinicke[1], M. Dukalski[2], and K. Wapenaar[3]

ABSTRACT

The reflection response of strongly scattering media often contains complicated interferences between primaries and (internal) multiples, which can lead to imaging artifacts unless handled correctly. Internal multiples can be kinematically predicted, for example by the Jakubowicz method or by the inverse scattering series (ISS), as long as monotonicity, that is, "correct" temporal event ordering, is obeyed. Alternatively, the (conventional) Marchenko method removes all overburden-related wavefield interactions by formulating an inverse problem that can be solved if the Green's and the so-called focusing functions are separable in the time domain, except for an overlap that must be predicted. For acoustic waves, the assumptions of the aforementioned methods are often satisfied within the recording regimes used for seismic imaging. However, elastic media support wave propagation via coupled modes that travel with distinct velocities. Compared to the acoustic case, not only does the multiple issue become significantly more severe, but also violation of monotonicity becomes much more likely. By quantifying the assumptions of the conventional Marchenko method and the ISS, unexpected similarities as well as differences between the requirements of the two methods come to light. Our analysis demonstrates that the conventional Marchenko method relies on a weaker form of monotonicity. However, this advantage must be compensated by providing more prior information, which in the elastic case is an outstanding challenge. Rewriting, or remixing, the conventional Marchenko scheme removes the need for prior information but leads to a stricter monotonicity condition, which is now almost as strict as for the ISS. Finally, we introduce two strategies on how the remixed Marchenko solutions can be used for imperfect, but achievable, demultiple purposes.

INTRODUCTION

In seismic exploration, structural images are often derived from a single-sided reflection response. However, traditional imaging methods assume single-scattering reflections (primaries only), such that other events, in particular multiples, create artifacts, which can be significant when the imaging target is buried under a strongly scattering overburden. In elastic media, this problem is worse: each interface couples compressional (P) and shear (S) waves, increasing the number of (unwanted) events drastically. Additionally, due to different propagation speeds of elastic modes, the (converted) primaries associated with an individual reflector arrive at different times, distributing information about this reflector in time. Hence, imaging artifacts can arise not only from (converted) multiples but also from converted primaries, that is, forward-scattered waves. Reflection data-driven methods are not (yet) capable of predicting forward scattering, but they are theorized to be able to handle (converted) multiples.

Wave-equation-based demultiple methods, such as Jakubowicz (1998), or the inverse scattering series (ISS, Weglein et al., 1997), predict and adaptively subtract internal multiples under two assumptions:

1) that the temporal ordering of primaries corresponds to the reflector ordering in depth, and
2) that internal multiples are recorded after their generating primaries (i.e., primaries associated with the internal multiple generators),

where temporal order refers to the vertical traveltime. These requirements, known as *monotonicity conditions*, are satisfied for

Manuscript received by the Editor 29 October 2019; revised manuscript received 29 April 2020; published ahead of production 05 June 2020; published online 11 September 2020.
[1]Delft University of Technology, Department of Geoscience and Engineering, Stevinweg 1, 2628CN Delft, The Netherlands and Aramco Overseas Company B.V., Informaticalaan 6-12, 2628ZD Delft, The Netherlands. E-mail: chris.reinicke@aramcooverseas.com.
[2]Aramco Overseas Company B.V., Informaticalaan 6-12, 2628ZD Delft, The Netherlands.
[3]Delft University of Technology, Department of Geoscience and Engineering, Stevinweg 1, 2628CN Delft, The Netherlands.

acoustic waves, except for special cases shown by Nita and Weglein (2009). In elastic media, however, violation of monotonicity becomes much easier because of mode conversions (Sun and Innanen, 2019).

A Marchenko-equation-based alternative for acoustic waves allows removal of all internal multiples associated with an entire group of layers at once, *without adaptive subtraction* (Broggini et al., 2012; Wapenaar et al., 2013; Slob et al., 2014). This method formulates an inverse problem with two equations (derived from reciprocity theorems) and four unknowns: the up- and downgoing Green's functions as well as the so-called up- and downgoing focusing functions. Numerous studies on the topic feature the Green's and focusing functions, which are separable in the time domain, except for an unavoidable overlap (χ_+). Given this overlap, two unknowns can be eliminated by muting. Subsequently, two coupled Marchenko equations are obtained and solved for the focusing functions, which, once found, yield the Green's functions. Eventually, upon multidimensional deconvolution of the retrieved Green's functions, overburden-related scattering interactions, including internal multiples, can be removed. We refer to this approach as the *conventional Marchenko method*.

The elastodynamic extension of the Marchenko method bears several challenges. First, speed differences between modes can lead to a second overlap (χ_-), which to date cannot be predicted without knowing the medium and only vanishes conditionally. Second, the previously mentioned unavoidable overlap (χ_+) between the Green's and the focusing functions is no longer easily predictable without additional constraints or significantly more prior information (Wapenaar and Slob, 2015). Similar restrictions have been encountered by prior work on inverse scattering of coupled modes. Nevertheless, these cases ignore the overlaps, either by assuming sufficiently small velocity differences between modes (Zakharov and Shabat, 1973; Bava and Ghione, 1984) or by excluding coupling (Ware and Aki, 1969).

To overcome the challenge related to the overlap χ_+, we derive a remixed, as opposed to the above-mentioned conventional, Marchenko method: the Green's and focusing functions are transformed such that the unavoidable, highly complex, overlap (χ_+) remixes into a trivial one. This strategy can be seen as a combination and generalization of the Marchenko schemes by van der Neut and Wapenaar (2016) and Dukalski et al. (2019).

The Marchenko method uses the aforementioned assumptions about the overlaps to separate the Green's functions from the focusing functions. To date, these requirements have not been sufficiently investigated and have not been compared to the monotonicity conditions of the ISS. Moreover, the requirements of the Marchenko method and the ISS are only formulated verbally, which makes a direct comparison of the requirements difficult. Therefore, we quantify these assumptions in a form of medium, angle of incidence, and redatuming depth dependent *separability conditions*. This analysis demonstrates that the monotonicity assumptions of the ISS are very similar to, but stricter than, the separability condition of the conventional Marchenko method. After remixing, the Marchenko method can be applied without prior medium information (no need for the overlap χ_+). Although, compared to the conventional Marchenko scheme, the separability condition becomes stricter, it still remains slightly more relaxed than the monotonicity assumption (1) of the ISS. This advantage of the (remixed) Marchenko method comes from handling the overburden as one complex multiple generator, rather than a stack of independent multiple generators.

Finally, we demonstrate how the solutions of the remixed Marchenko method can be used to remove internal multiples that postdate their generating primaries. In contrast to the ISS, which encounters the same limitation, see assumption (2), the remixed Marchenko method tracks the error caused by the remaining internal multiples. This tracked error is expected to persist in field data studies (Ravasi et al., 2016; Staring et al., 2018), but it could be eliminated by transforming the remixed solutions back to the conventional ones, using energy conservation and the minimum-phase property of the focusing function, similar to Dukalski et al. (2019). The latter strategy relies on the reconstruction of a minimum-phase matrix from its normal product, which is subject to ongoing research and will be published elsewhere.

This paper is structured as follows. First, we briefly outline the conventional Marchenko scheme, quantify its assumptions as a separability condition, and interpret the required initial estimate. Second, we derive the remixed Marchenko scheme, which leads to a stricter separability condition. Third, we quantify the monotonicity conditions of the ISS, which we compare to the requirements of the aforementioned (remixed) Marchenko method. Finally, we illustrate our findings with numerical examples. In this analysis, we assume that surface-related multiples are removed during preprocessing, and, thus, we use the terms multiples and internal multiples interchangeably. Although we consider the simplest yet a nontrivial case, horizontally layered elastic media, our analysis is already highly relevant for the Middle East (El-Emam et al., 2001; Reinicke et al., 2019), and it extends qualitatively to more general cases.

Notation

We consider 2D lossless horizontally layered elastic media in the *x*-*z* coordinates. According to Snell's law, horizontal slownesses s_x (i.e., horizontal ray-parameter) are conserved according to

$$s_x = \frac{\sin(\alpha_{P/S}(z))}{c_{P/S}(z)} = \text{constant}, \tag{1}$$

where the subscripts refer to P- and S-waves. Further, $\alpha_{P/S}$ and $c_{P/S}$ are the propagation angle with respect to the vertical axis (z) and the propagation velocity, respectively. A representation in the horizontal-slowness intercept-time domain (s_x, τ) allows separation of 2D wavefields $U(x, z, t)$ into a set of decoupled 1D wavefields

$$U(s_x, z, \tau) = \int_{-\infty}^{\infty} U(x, z, \tau + s_x x)\mathrm{d}x. \tag{2}$$

In this paper, we use the terms time and intercept time interchangeably; that is, the entire analysis considers the vertical traveltime, *as opposed to* the total traveltime.

We restrict our analysis to propagating waves, that is, $|s_x| \leq 1/c_P$ (assuming $c_P > c_S$), and we neglect measurement-induced limitations, such as a finite bandwidth, because here we wish to focus on a fundamentally physical (not measurement-borne) limitation. Further, we work with P- and S- one-way wavefields (Frasier, 1970; Ursin, 1983), organized in 2×2 matrices per discrete horizontal slowness and time as

$$\mathbf{U}(s_x, z, \tau) = \begin{pmatrix} U_{PP} & U_{PS} \\ U_{SP} & U_{SS} \end{pmatrix}(s_x, z, \tau). \tag{3}$$

The elements of the arbitrary wavefield $\mathbf{U}(s_x, z, \tau)$ are associated with source- (the second subscript) and receiver-side (the first subscript) wavefield potentials (P and S).

Finally, we introduce a detail-hiding notation that omits coordinates and implies temporal convolutions when two matrices $\mathbf{U}_1$ and $\mathbf{U}_2$ are multiplied; for example, $\mathbf{U}_1\mathbf{U}_2$ stands for

$$\int_{-\infty}^{\infty} \mathbf{U}_1(s_x, z, \tau - \tau')\mathbf{U}_2(s_x, z, \tau')\mathrm{d}\tau'. \tag{4}$$

MARCHENKO GREEN'S FUNCTION RETRIEVAL

Suppose all of the multiples due to the overburden above the redatuming depth z_i shall be removed. For this purpose, we might use the Green's functions, $\mathbf{G}^{-,+}(s_x, z_0, z_i, \tau)$ and $\mathbf{G}^{-,-}(-s_x, z_0, z_i, \tau)$, associated with downward- "+" and upward- "−" radiating sources (the second superscript) at the redatuming depth z_i, respectively, and recordings of upgoing waves "−" (the first superscript) at acquisition level z_0 (see Figure 1). From these Green's functions, a redatumed reflection response $\mathbf{R}_{rd}(s_x, z_i, \tau)$, free of overburden-related scattering, can be obtained by solving

$$\mathbf{G}^{-,+} = -\boldsymbol{\sigma}_z\mathbf{G}^{-,-}\mathbf{R}_{rd}^{\mathrm{T}}\boldsymbol{\sigma}_z, \tag{5}$$

via an Amundsen (2001) deconvolution. Here, we exploit wavefield symmetries in horizontally layered media by means of a transpose in the P-S space (superscript "T") and through the diagonal matrix $\boldsymbol{\sigma}_z = \mathrm{diag}[\delta(\tau), -\delta(\tau)]$, where $\delta(\tau)$ is a temporal delta spike. These symmetries allow us to proceed with the retrieved Green's functions $\mathbf{G}^{-,\pm}$, although they are associated with horizontal slownesses s_x of the opposite sign (a derivation can be found in Appendix A). The challenge is to retrieve these Green's functions from a reflection response $\mathbf{R}(s_x, z_0, \tau)$ recorded at a scattering-free surface z_0 at the top, which can be accomplished by a Marchenko method.

First, we highlight the underlying assumptions and the prior information required by the conventional Marchenko method. Second, we provide a physical interpretation of the prior information, and, finally, we propose an alternative Marchenko formulation, which trades prior information for stricter assumptions. It will be shown that the conventional Marchenko method as well as its alternative formulation rely on separability conditions, which we express quantitatively. In the next section, this quantification will allow us to compare the requirements of the Marchenko method to those of the ISS.

Quantitative separability condition

We briefly outline the elastodynamic Marchenko method, derived by one of the authors (Wapenaar, 2014), and we quantify the assumptions as a separability condition.

Instead of predicting multiples by combining all possible triplets of primaries associated with the overburden (Coates and Weglein, 1996), the Marchenko method solves an inverse problem formed by two equations, the convolution- and correlation-type representation theorems

$$\mathbf{G}^{-,+} + \mathbf{F}_1^- = \mathbf{R}\mathbf{F}_1^+, \tag{6}$$

$$(\mathbf{G}^{-,-})^* + \mathbf{F}_1^+ = \mathbf{R}^\dagger\mathbf{F}_1^-, \tag{7}$$

with four unknowns: the Green's functions $\mathbf{G}^{-,\pm}$ and the focusing functions $\mathbf{F}_1^\pm(s_x, z_0, z_i, \tau)$. The latter ones are defined in a truncated medium that is identical to the overburden, but scattering-free above z_0 and below z_i. The superscripts denote a time reversal (∗) and a time reversal combined with a transpose in the P-S space (†). Further, an illustration of equations 6 and 7 can be found in Figure 1 for an acoustic medium and in Figures 2a and 3a for an elastic medium.

In an attempt to constrain equations 6 and 7, two temporal projectors $\mathbf{P}^\pm$ are applied as a Hadamard matrix product in the P-S space (details about the projectors can be found in Appendix B). In other publications, the projectors also are referred to as window functions; both terms describe exactly the same operator. Without loss of generality, the projectors preserve the focusing functions, but mute the Green's functions, except for the temporal overlaps, $\mathbf{P}^-[\mathbf{G}^{-,+}] = \boldsymbol{\chi}_-$ and $\mathbf{P}^+[(\mathbf{G}^{-,-})^*] = \boldsymbol{\chi}_+$, such that equations 6 and 7 simplify to

$$\boldsymbol{\chi}_- + \mathbf{F}_1^- = \mathbf{P}^-[\mathbf{R}\mathbf{F}_1^+], \tag{8}$$

$$\boldsymbol{\chi}_+ + \mathbf{F}_1^+ = \mathbf{P}^+[\mathbf{R}^\dagger\mathbf{F}_1^-]. \tag{9}$$

Note that keeping the overlap $\boldsymbol{\chi}_-$ explicit will lead to key insights of this paper. The solution strategy hopes that the overlaps $\boldsymbol{\chi}_\pm$ can be estimated such that the inverse problem resembles a set of coupled Marchenko equations that can be solved recursively as

$$\mathbf{F}_1^+ = \sum_{k=0}^{\infty} \boldsymbol{\Xi}_k \quad \text{with } \boldsymbol{\Xi}_k = \mathbf{P}^+[\mathbf{R}^\dagger\mathbf{P}^-[\mathbf{R}\boldsymbol{\Xi}_{k-1}]], \tag{10}$$

using $\boldsymbol{\Xi}_0 = -\boldsymbol{\chi}_+ - \mathbf{P}^+[\mathbf{R}^\dagger\boldsymbol{\chi}_-]$ as the initial estimate, and assuming convergence of the series (which has been shown for the acoustic case, Dukalski and de Vos, 2017). From the retrieved solution $\mathbf{F}_1^+$, the remaining unknowns can be constructed.

Estimating the overlaps remains very challenging. To proceed, the Marchenko method first assumes that $\boldsymbol{\chi}_-$ is a null matrix $\mathbf{O}$, and, second, that it requires $\boldsymbol{\chi}_+$ as prior information (a physical interpretation of $\boldsymbol{\chi}_+$ follows in the next subsection).

The assumption $\boldsymbol{\chi}_- = \mathbf{O}$ demands that the focusing function $\mathbf{F}_1^-$ and the Green's function $\mathbf{G}^{-,+}$ remain separable in the time domain (see the $\mathbf{F}_1^-/\mathbf{G}^{-,+}$ separability in Figures 1a and 2a). Although true for 1.5D acoustic media, this assumption can be violated in 1.5D elastic media (see Figure 2b), and it only holds under the $\boldsymbol{\chi}_-$-separability-condition

$$\sum_{k=1}^{i-1} \Delta z^{(k)}(s_{z,\mathrm{S}}^{(k)} - s_{z,\mathrm{P}}^{(k)}) < 2\Delta z^{(i)} s_{z,\mathrm{P}}^{(i)}, \tag{11}$$

which we derive in Appendix B. Variables $\Delta z^{(k)}$ and $s_{z,\mathrm{P/S}}^{(k)}$ denote the thickness and the vertical slownesses of P- and S-waves in the kth layer, respectively (the layer labeling is depicted in Figure 5a). The right side of equation 11 describes the two-way traveltime of a P-wave through the ith layer (embedding the redatuming level), and the left side is the one-way traveltime difference between a P- and an S-wave propagating from the shallowest to the deepest interface of the overburden. Note that the separability condition becomes stricter if identical projectors $\mathbf{P}^+ = \mathbf{P}^-$ are used.

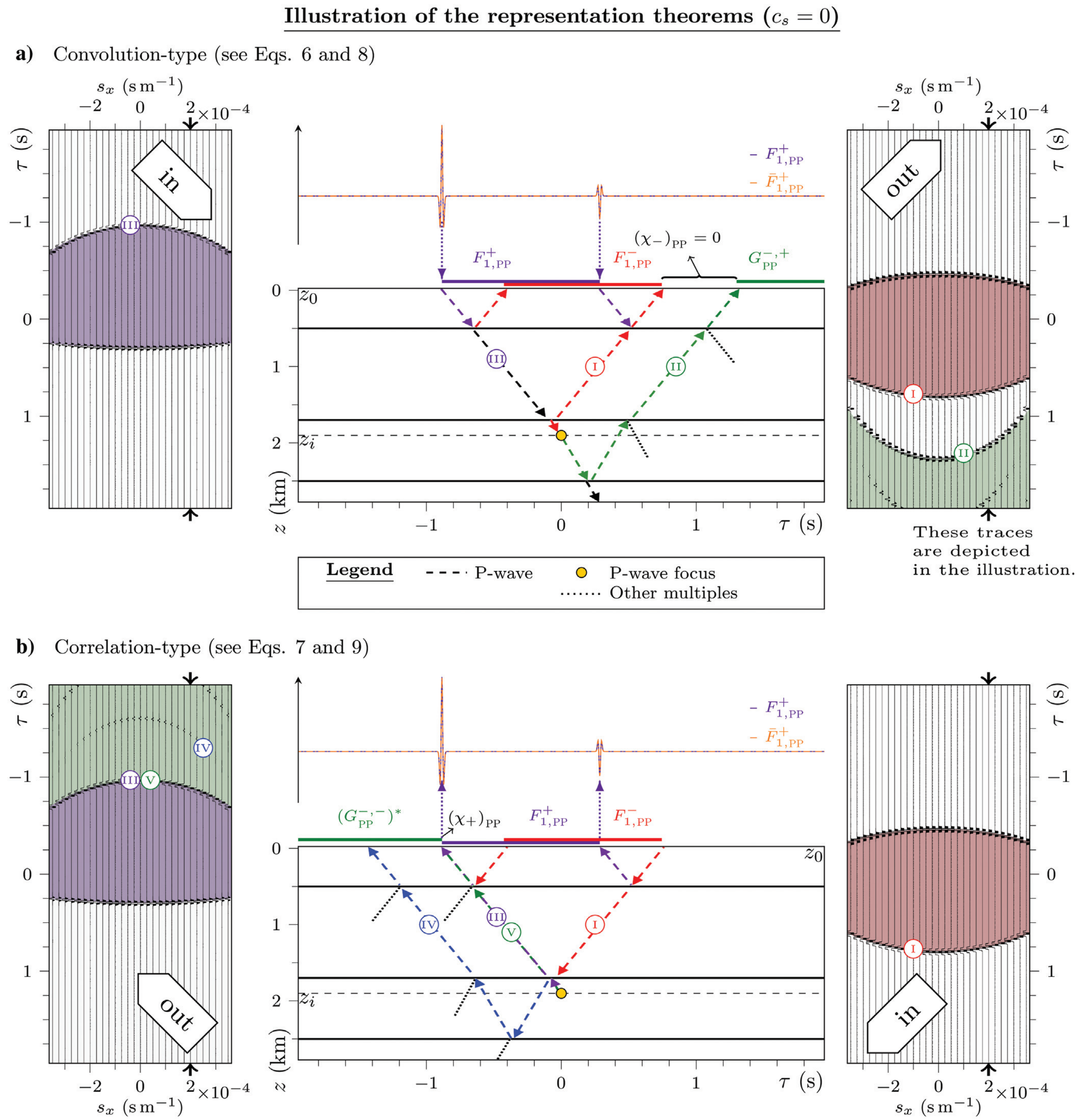

Figure 1. Illustration of the (a) convolution- and (b) correlation-type representation theorems. This figure depicts an acoustic experiment to help the interpretation of the elastic experiments shown in Figures 2 and 3. The representation theorems describe a scattering experiment: special fields (the focusing functions $\mathbf{F}_1^{\pm}$) are injected into a medium (see the arrows labeled "in"), the arrow diagram in the center depicts the scattering paths for a single horizontal slowness s_x (marked with black arrows in the s_x-τ gathers), and another special field scatters back to the recording surface z_0 (see the arrows labeled "out"). Note that all wavefields are consistently color coded in Figures 1–3. The scattering of $\mathbf{F}_1^+$ [violet in panel (a)] and $\mathbf{F}_1^-$ [red in panel (b)] by a (a) time-forwarding and (b) time-reversing medium results in superpositions of focusing and Green's functions $\mathbf{F}_1^- + \mathbf{G}^{-,+}$ and $\mathbf{F}_1^+ + (\mathbf{G}^{-,-})^*$, respectively. The top trace shows the true (violet) and retrieved (orange) focusing functions $F^+_{1,\mathrm{PP}}$ and $\bar{F}^+_{1,\mathrm{PP}}$, respectively. The last event of $\mathbf{F}_1^-$ (event I) and the first event of $\mathbf{G}^{-,+}$ (event II) are represented by the red and green paths, respectively (also see the s_x-τ gathers). Similarly, the first event of $\mathbf{F}_1^+$ (event III) and the last event of $(\mathbf{G}^{-,-})^*$ (event V) are highlighted by the violet and green travel paths, respectively. The fastest multiple coda of $(\mathbf{G}^{-,-})^*$ (event IV) propagates along the blue path. At the recording surface z_0, the overlap between focusing and Green's functions only contains a direct wave (events III and V). The overlap(s) between focusing and Green's functions appear to have a trivial s_x-dependency (illustrated by the s_x-τ gathers); however, this will change in the elastic case (see Figure 2). For illustration purposes, all responses are convolved with a 30 Hz Ricker wavelet. Medium parameters can be found in Appendix C.

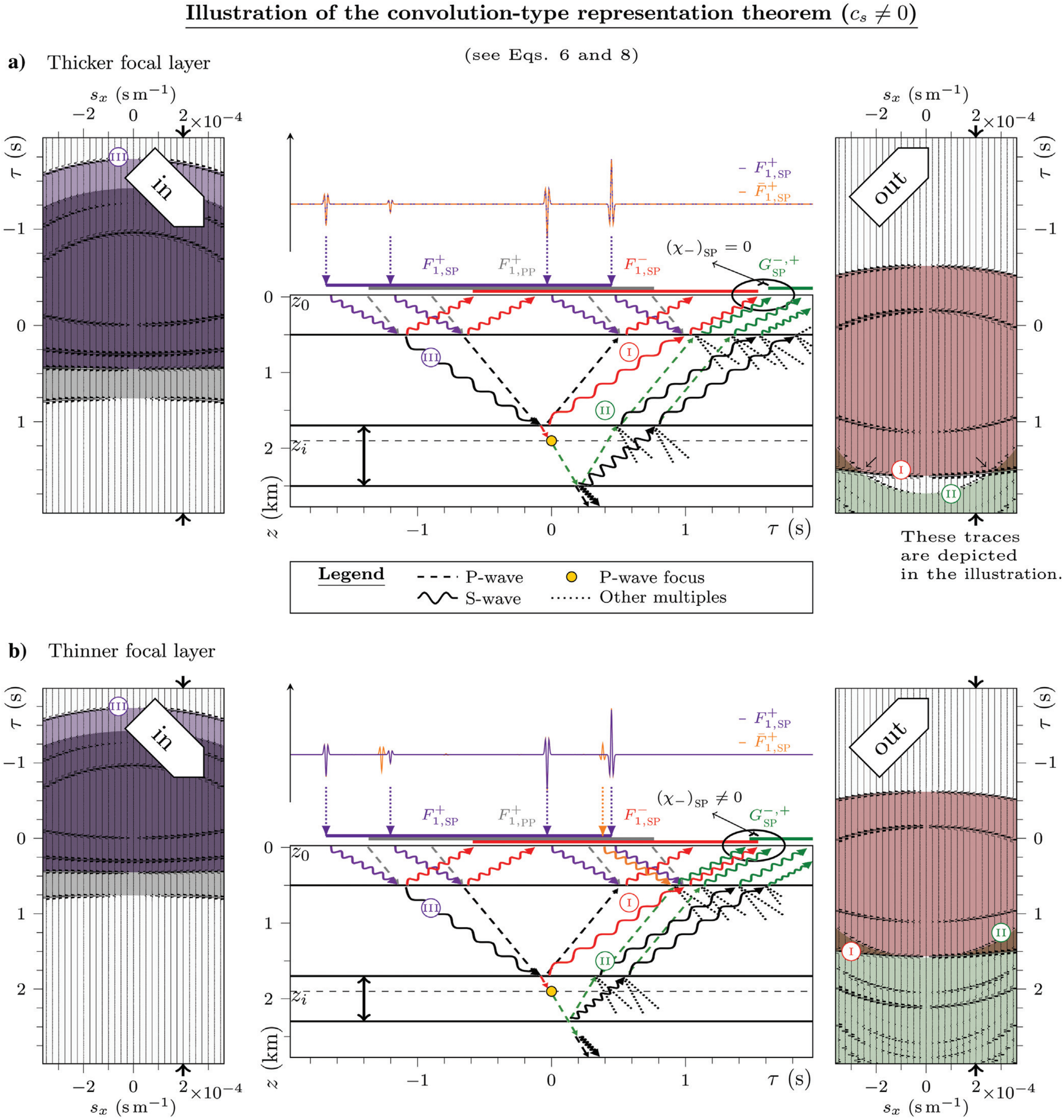

Figure 2. (a) Idem as Figure 1a for the same medium supporting elastic wave propagation (arbitrarily chosen SP component shown). Compared to the acoustic experiment shown in Figure 1a, the number of scattering paths increased drastically because at each interface the injected wavefield is reflected and transmitted as P- and S-waves. Moreover, creation of a P-wave focus requires injection of P- (the gray color for $F^+_{1,\mathrm{PP}}$) and S-waves (the violet color for $F^+_{1,\mathrm{SP}}$). Due to the mode coupling, the $\mathbf{F}_1^-/\mathbf{G}^{-,+}$ separability is only violated for sufficiently large horizontal slownesses, $|s_x| > 2.54 \times 10^{-4}$ sm^{-1} (indicated by the black arrows inside the top-right s_x-τ gather). For smaller horizontal slownesses, the separability conditions (see equations 11 and 12) are satisfied and the Marchenko method retrieves the correct focusing function (see the top trace). (b) Idem as panel (a), except that the thickness of the focusing layer is reduced such that the first event of $G^{-,+}_{\mathrm{SP}}$ (event II) predates the last event of $F^-_{1,\mathrm{SP}}$ (event I), leading to a temporal overlap (see the black ellipse in the illustration and the red-green area overlap in the s_x-τ gathers). If we erroneously assume zero overlap $\boldsymbol{\chi}_- = \mathbf{O}$, the Marchenko method forces the overlapping part of the Green's function to become part of the upgoing focusing function $\bar{\mathbf{F}}_1^-$. As a result, the retrieved downgoing focusing function $\bar{\mathbf{F}}_1^+$ contains an artifact (see the orange arrow) that cancels a multiple generated by event II. The other artifacts of the retrieved focusing function $\bar{\mathbf{F}}_1^+$ (e.g., approximately $\tau = -1.25$ s) are caused by similar mechanisms but are not immediately easy to interpret here.

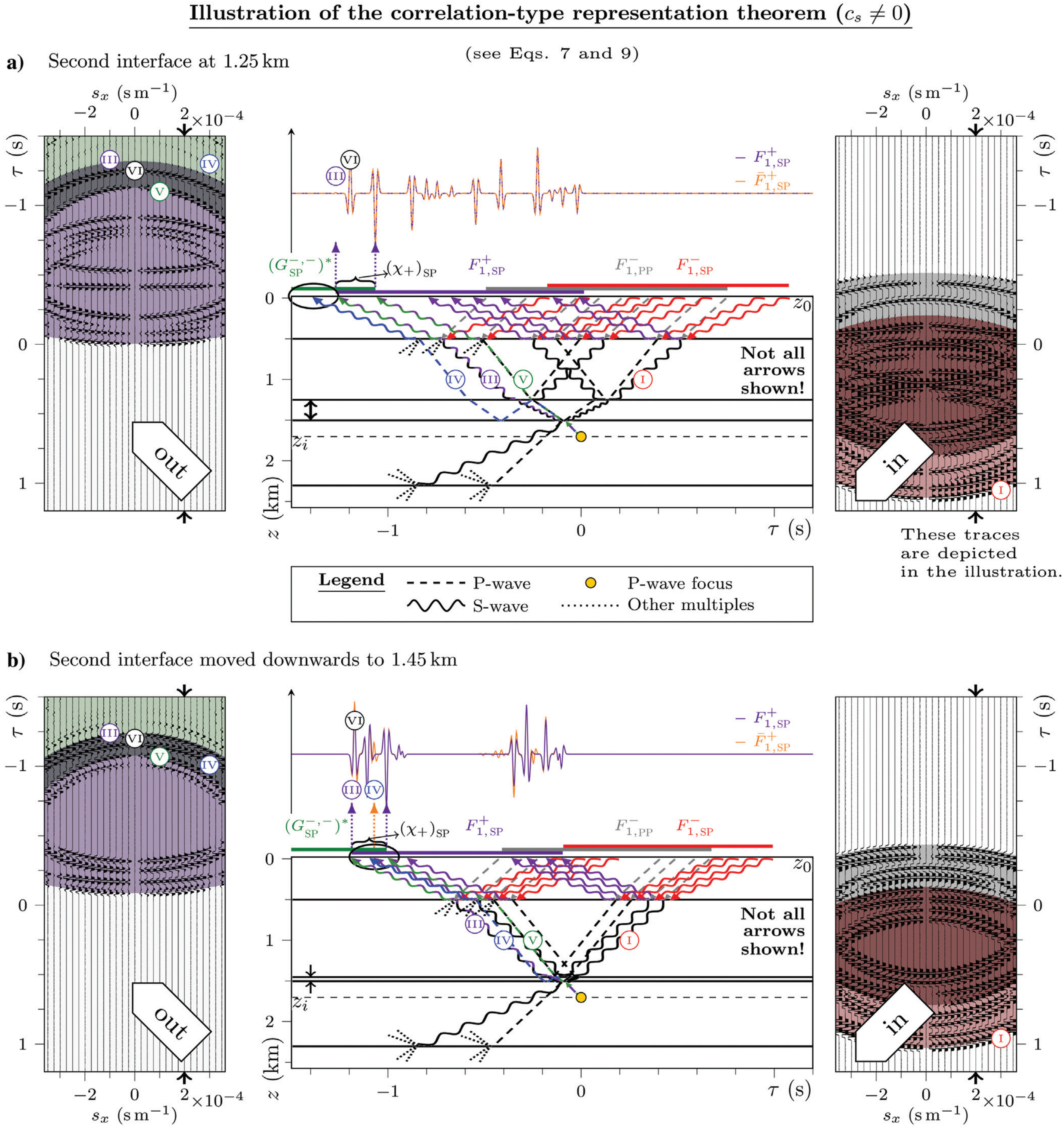

Figure 3. (a) Idem as Figure 1b but now the medium is elastic and contains an additional interface (an arbitrarily chosen SP component is shown). Because the additional layer generates so many extra events, we do not draw all paths in the illustration. In contrast to the acoustic case in Figure 1b, creation of a P-wave focus requires injection of P- (the gray color is for $F^-_{1,\mathrm{PP}}$) and S-waves (the red color is for $F^-_{1,\mathrm{SP}}$). Due to P-S coupling at each interface, the overlap χ_+, which is bounded by the first event of $\mathbf{F}^+_1$ (event III) and the last event of $(\mathbf{G}^{-,-})^*$ (event V), contains not only a direct wave but all forward-scattered waves. The s_x-τ gather shows that the temporal separation between forward-scattered waves (e.g., events III, V, and VI) and multiples (e.g., event IV) decreases with the increasing horizontal slowness. (b) Idem as Figure 3a, except that the second interface from above has been moved downward, creating a thinner layer (the layer thickness is reduced from 250 to 50 m). As a result, the overlap χ_+ contains not only the forward-scattered waves but also fast multiples (see event IV in the ellipse). Approximating the overlap χ_+ only by forward-scattered waves, that is, ignoring fast multiples such as event IV, leads to an erroneous focusing function $\bar{\mathbf{F}}^+_1$ (see the orange and violet traces for comparison). Errors occur not only within the temporal extent of the overlap χ_+ but also at other times.

Physical interpretation of the overlap χ_+

In 1.5D acoustic media, the overlap χ_+ is a direct wave propagating from the redatuming level z_i to the acquisition surface z_0. Wapenaar and Slob (2015) demonstrate that, in elastic media, the unavoidable overlap χ_+ does not simply consist of direct P- and S-waves, but of all waves that forward scatter from the redatuming level z_i to the acquisition surface z_0 (such as events III and V in Figures 1b and 3a). This interpretation is a special case. In general, a multiple coda propagating mainly as P-wave may outpace forward-scattered waves propagating mainly as S-waves; for example, see events IV and III in Figure 3b, respectively. These multiple-coda events become part of the overlap χ_+, and we refer to them as *fast multiples*. The occurrence of fast multiples is prevented if the χ_+-separability-condition

$$\sum_{k=1}^{i-1} \Delta z^{(k)} (s_{z,\mathrm{S}}^{(k)} - s_{z,\mathrm{P}}^{(k)}) < 2 \, \min\{\Delta z^{(k)} s_{z,\mathrm{P}}^{(k)} | k \in [1, i]\} \quad (12)$$

holds (derived in Appendix B). The minimum function $\min\{\cdot\}$ selects the smallest element of the given set, which in this case is the delay between the fastest multiple coda and the corresponding forward-scattered wave propagating from z_i to z_0.

If the separability condition in equation 12 is violated, the conventional Marchenko method requires the fast multiples as prior information. Even in the special case in which equation 12 holds such that the overlap χ_+ simplifies to only forward-scattered waves, it still consists of 2^{n-1} events per elastic component, where n is the number of reflectors inside the overburden. Thus, finding the initial estimate χ_+ without further constraints appears very unrealistic for an unknown model.

Marchenko method with trivial initial estimate

In this section, we modify the conventional Marchenko scheme to remove the need for prior information contained by χ_+ in exchange for a stricter separability condition.

We exploit the freedom to convolve the representation theorems in equations 6 and 7 with an arbitrary time-dependent matrix $\mathbf{B}(s_x, z_i, z_0, \tau)$ from the right as

$$\mathbf{U}^{-,+} + \mathbf{V}_1^- = \mathbf{R}\mathbf{V}_1^+, \quad (13)$$

$$(\mathbf{U}^{-,-})^* + \mathbf{V}_1^+ = \mathbf{R}^\dagger \mathbf{V}_1^-, \quad (14)$$

where we introduce $\mathbf{V}_1^\pm = \mathbf{F}_1^\pm \mathbf{B}$, $\mathbf{U}^{-,+} = \mathbf{G}^{-,+}\mathbf{B}$, and $\mathbf{U}^{-,-} = \mathbf{G}^{-,-}\mathbf{B}^*$. This approach allows us to arrive at a different set of equations and can be interpreted as a form of preconditioning (Dukalski and de Vos, 2017). Like Dukalski et al. (2019), Mildner et al. (2019), and Elison et al. (2020), we assume an unknown, although later recoverable, $\mathbf{B}$, contrary to other authors who use a known $\mathbf{B}$ (van der Neut and Wapenaar, 2016; Meles et al., 2018; Reinicke et al., 2018).

Next, we define the unknown $\mathbf{B}$ such that the overlap χ_+ unfolds onto an identity. This strategy can be seen as applying an unknown transformation (convolution with $\mathbf{B}$) that maps the typically unknown initial guess χ_+ onto a trivial one. As a result, the solutions also are transformed from $\mathbf{F}_1^\pm$ to $\mathbf{V}_1^\pm = \mathbf{F}_1^\pm \mathbf{B}$. We emphasize that operator $\mathbf{B}$ is not a mere time shift as in the acoustic scheme by van der Neut and Wapenaar (2016), nor is it a form of a wavelet as in the scheme by Dukalski et al. (2019) and Elison et al. (2020), but it is a much more general matrix filter. Now, equation 14 can be easily separated as

$$\mathbf{P}_B^+[(\mathbf{U}^{-,-})^*] = \chi_+^B = \mathbf{I}, \quad (15)$$

$$\mathbf{P}_B^+[\mathbf{V}_1^+] = \mathbf{V}_1^+, \quad (16)$$

where $\mathbf{I}$ is an identity matrix multiplied by a temporal delta function. Note that projector $\mathbf{P}_B^+$ can be very different from projector $\mathbf{P}^+$ in equation 9 (details about the projectors can be found in Appendix B). After applying a projector to equation 13, such that

$$\mathbf{P}_B^-[\mathbf{U}^{-,+}] = \chi_-^B, \quad (17)$$

$$\mathbf{P}_B^-[\mathbf{V}_1^-] = \mathbf{V}_1^-, \quad (18)$$

we can simplify equations 13 and 14 to

$$\chi_-^B + \mathbf{V}_1^- = \mathbf{P}_B^-[\mathbf{R}\mathbf{V}_1^+], \quad (19)$$

$$\mathbf{I} + \mathbf{V}_1^+ = \mathbf{P}_B^+[\mathbf{R}^\dagger \mathbf{V}_1^-]. \quad (20)$$

Compared to equations 8 and 9, the overlaps $\chi_\pm$ are *remixed* into χ_-^B and $\chi_+^B = \mathbf{I}$; thus, we refer to $\mathbf{B}$ as the remixing operator. For the special case in which the remixed overlap χ_-^B remains zero, we can retrieve remixed solutions

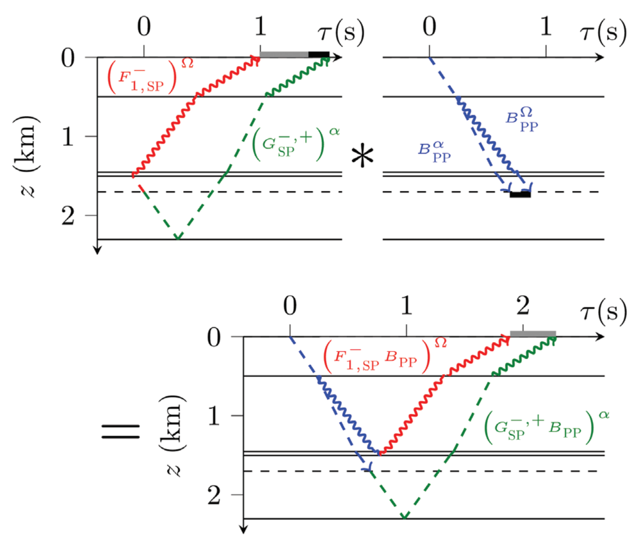

Figure 4. Effect of remixing on temporal separation, illustrated analogously to Figures 2 and 3. Remixing reduces the temporal distance between $\mathbf{F}_1^-$ and $\mathbf{G}^{-,+}$ (see the gray and black bar) by the duration of the remixing operator (see the black bar). We depict the first (superscript α) and last (superscript Ω) events of $\mathbf{F}_1^-$ (red), $\mathbf{G}^{-,+}$ (green), and $\mathbf{B}$ (blue). The traveltimes of the first and the last events of $\mathbf{B}$ are derived in Appendix B.

$$\mathbf{V}_1^+ = \sum_{k=0}^{\infty} \mathbf{\Xi}_k, \quad \text{with } \mathbf{\Xi}_k = \mathbf{P}_B^+[\mathbf{R}^\dagger \mathbf{P}_B^-[\mathbf{R}\mathbf{\Xi}_{k-1}]] \tag{21}$$

using a trivial initial estimate $\mathbf{\Xi}_0 = -\chi_+^B$. Further onwards, we will introduce a demultiple strategy that only requires the resulting remixed Green's functions $\mathbf{U}^{-,\pm}$ as input.

The advantage of a trivial initial estimate, $\chi_+^B = \mathbf{I}$, comes at a cost: although unknown, the remixing operator is associated with a source at the surface at z_0 and a receiver at the redatuming depth z_i. Thus, $\mathbf{B}$ moves the focal point to the acquisition surface. This process reduces the temporal separation between the focusing function $\mathbf{F}_1^-$ and the Green's function $\mathbf{G}^{-,+}$ by the temporal extent of the remixing operator (see Figure 4). As a result, an originally zero overlap $\chi_- = \mathbf{O}$ can become nonzero, $\chi_-^B \neq \mathbf{O}$. This is because the remixed Marchenko method relies on the χ_-^B separability condition (a derivation can be found in Appendix B)

$$\sum_{k=1}^{i-1} \Delta z^{(k)} (s_{z,\mathrm{S}}^{(k)} - s_{z,\mathrm{P}}^{(k)}) < \Delta z^{(i)} s_{z,\mathrm{P}}^{(i)}, \tag{22}$$

which is stricter than the χ_--separability-condition of the conventional Marchenko method (see equation 11). The effect of satisfying, or violating, the aforementioned separability conditions is summarized in Table 1.

MONOTONICITY CONDITIONS OF THE ISS

The ISS relies on monotonicity assumptions (1) and (2) (see the "Introduction" section), which, to the best of our knowledge, have always been formulated verbally. We quantify these assumptions in the form of two inequalities. Subsequently, we compare them against the conventional and remixed Marchenko methods.

Quantifying monotonicity in terms of separability conditions

Consistent with the previous section, we aim to remove multiples related to the overburden above z_i. Monotonicity assumption (1) in the introduction requires that the P-wave traveltime through each layer inside the overburden is sufficiently long to separate the (converted) primaries of adjacent reflectors in time (compare Figure 5a and 5b), and it must hold for each elastic component. This requirement can be formulated as a separability condition (derived in Appendix B)

$$\sum_{k=1}^{j-1} \Delta z^{(k)} (s_{z,\mathrm{S}}^{(k)} - s_{z,\mathrm{P}}^{(k)}) < \Delta z^{(j)} s_{z,\mathrm{P}}^{(j)}, \quad \forall\, j \in [2, i]. \tag{23}$$

Monotonicity assumption (2) states that multiples are recorded after their generating primaries and can be formulated as (derived in Appendix B)

$$\sum_{k=1}^{i-1} \Delta z^{(k)} (s_{z,\mathrm{S}}^{(k)} - s_{z,\mathrm{P}}^{(k)}) < \min\{\Delta z^{(k)} s_{z,\mathrm{P}}^{(k)} | k \in [1, i]\}. \tag{24}$$

Violating monotonicity causes erroneous multiple predictions at the arrival times of the primaries (e.g., see Figure 16 in Sun and Innanen, 2019). Subsequent match subtraction of the mispredicted multiples may affect the primaries.

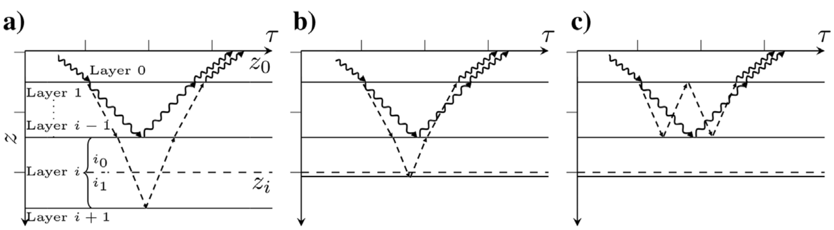

Figure 5. Two primary reflections (an arbitrarily chosen SS component) that (a) obey and (b) violate monotonicity assumption (1). (c) A multiple that predates a primary of one of its generators, violating monotonicity assumption (2). The dashed and sinusoidal lines represent the P- and S-waves, respectively. The layers are labeled with respect to the redatuming depth z_i.

Analysis of Marchenko and ISS separability conditions

Now, we compare the assumptions of the conventional and remixed Marchenko methods (see equations 11, 12, and 22) with the monotonicity assumptions of the ISS (see equations 23 and 24).

All of the aforementioned methods rely on separability conditions that have the same term on the left side. This term describes the traveltime difference between P- and S-waves propagating from the shallowest to the deepest reflector of the overburden. Hence, the likeli-

Table 1. A summary of the effect of satisfying and violating the separability conditions of the conventional and the remixed Marchenko method. The left side (l.s.) of all inequalities in this table is $\sum_{k=1}^{i-1} \Delta z^{(k)} (s_{z,\mathrm{S}}^{(k)} - s_{z,\mathrm{P}}^{(k)})$.

	Separability condition		Satisfied	Violated
Conventional	χ_- l.s. $< 2\Delta z^{(i)} s_{z,\mathrm{P}}^{(i)}$	(equation 11)	$\chi_- = \mathbf{O}$	$\chi_- \neq \mathbf{O}$ with finite duration
	χ_+ l.s. $< 2 \min\{\Delta z^{(k)} s_{z,\mathrm{P}}^{(k)} \| k \in [1, i]\}$	(equation 12)	χ_+ *only* contains forward-scattered waves	χ_+ contains forward-scattered waves *and* fast multiples
Remixed	χ_-^B l.s. $< \Delta z^{(i)} s_{z,\mathrm{P}}^{(i)}$	(equation 22)	$\chi_-^B = \mathbf{O}$	$\chi_-^B \neq \mathbf{O}$ with finite duration
	χ_+^B unconditionally (by definition $\chi_+^B = \mathbf{I}$)		$\chi_+^B = \mathbf{I}$	not applicable

hood of violating these separability conditions increases with depth and vertical slowness differences between the P- and S-waves $(s_{z,\mathrm{S}} - s_{z,\mathrm{P}})$.

The remixed Marchenko scheme and the ISS can be evaluated without prior medium information, which results in a fair comparison: the χ^B-separability-condition of the remixed Marchenko scheme is nearly identical to the monotonicity assumption (1) of the ISS (compare equations 22 and 23). However, the condition for the remixed Marchenko scheme (see equation 22) only needs to be obeyed by the redatuming layer i, rather than by each layer inside the overburden (see equation 23). For example, a sufficiently slim layer inside the overburden can be prohibitive for the ISS whereas the remixed Marchenko method can handle it as long as the redatuming layer i provides sufficient temporal support $\Delta z^{(i)} s^{(i)}_{\mathrm{S,P}}$. Hence, the requirement of the remixed Marchenko scheme, that is, the separability of $\mathbf{V}^-_1$ from $\mathbf{U}^{-,+}$, can be seen as a relaxed version of the monotonicity condition (1). This advantage of the (remixed) Marchenko method can be understood through the fundamentally different nature of the two algorithms: the ISS is applied in a fashion that scans through the data along the time, or (pseudo)depth, direction; that is, it treats the medium as a stack of individual multiple generators (although there is *no* need for identifying the generators). In contrast, the (remixed) Marchenko method exploits scattering relations between wavefields associated with a shallow and a deep part of the medium, where the separation between shallow and deep is arbitrary (Dukalski and de Vos, 2020). Once retrieved, these wavefields can be used to remove multiples generated by the shallow medium (i.e., the overburden). Thus, the overburden is handled as one complex multiple generator.

The χ_--separability-condition of the conventional Marchenko method is more relaxed (compare equations 11, 22, and 23). This relaxation emerges due to a missing factor of two on the left side of equation 11; that is, the conventional Marchenko scheme demands temporal separability in terms of the one- instead of the two-way traveltime ($\mathbf{F}^-_1 \leftrightarrow \mathbf{V}^-_1$ and $\mathbf{G}^{-,+} \leftrightarrow \mathbf{U}^{-,+}$). However, the more relaxed separability condition must be compensated by estimating the remaining overlap χ_+, that is, by providing prior information. Hence, the remixed Marchenko method trades prior information for a stricter assumption. This trade-off is not discussed by van der Neut and Wapenaar (2016) because they do not consider forward-scattered waves.

Further, elastic overburden removal through the ISS entails a high risk of violating the monotonicity assumption (2), which is quantified by equation 24: with increasing depth, the right side of the condition decreases or remains constant, whereas the left side increases. In other words, increasing the depth leads to a higher probability of fast multiples occurring, that is, multiples outpacing their generating primaries. Fast multiples also can be encountered by the conventional Marchenko method, which requires them to be included in the initial estimate. Again, due to the one- and two-way traveltimes, the occurrence of fast multiples in the conventional Marchenko method and the ISS differs by a factor of two (compare equations 12 and 24). The remixed Marchenko scheme encodes the effect of fast multiples in the remixing operator $\mathbf{B}$, which allows us to solve the scheme with a trivial initial estimate. However, the remixing operator remains in the retrieved solutions ($\mathbf{V}^{\pm}_1$ and $\mathbf{U}^{-,\pm}$). Hence, the remixed Marchenko scheme tracks, but does not remove, the impact of fast multiples (which will become obvious in equation 26 in the next section).

Note that the discussed separability conditions only consider the temporal event ordering, but they neglect the amplitudes of the events. Errors due to violating the separability conditions may be negligible close to zero-incidence where mode conversions are weak, but they become increasingly significant with the increasing angle of incidence.

Moreover, the separability conditions are domain-dependent. Among others, Sun and Innanen (2016) have addressed this issue in the context of the ISS. For Marchenko methods, the separation of focusing functions from the Green's functions typically is performed in the space-time domain (Wapenaar et al., 2014) or in the linear Radon domain (Slob et al., 2014). The separation in the latter domain is favorable, particularly in 1.5D media, because horizontal slownesses can be treated separately, reducing the risk of unwanted overlaps. It may be possible to relax the separability conditions further by considering another domain, which will be subject to future investigation.

DEMULTIPLE STRATEGIES FOR REMIXED MARCHENKO SCHEME

Now, we propose two demultiple strategies derived from the remixed Marchenko solutions. The first one only requires the remixed solutions but does not remove all of the overburden interactions. The second one aims to remove all of the overburden interactions

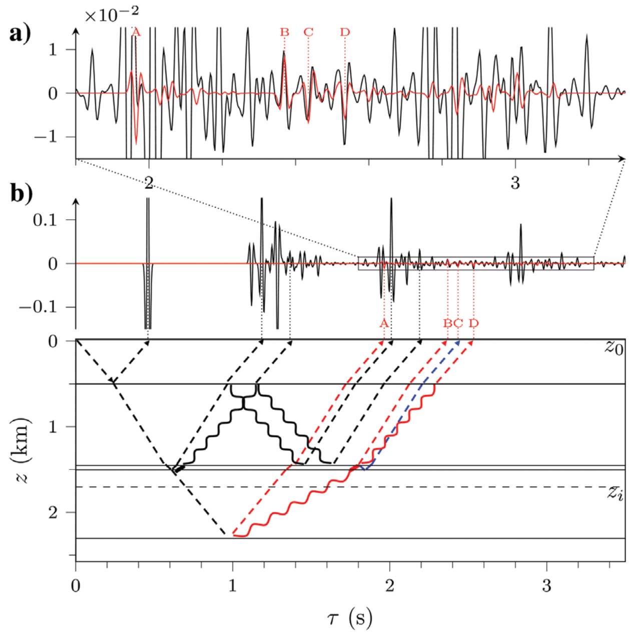

Figure 6. Reflection response (the black traces) and demultiple result (the red traces) according to equation 26 (arbitrarily chosen PP component, $s_x = 2 \times 10^{-4}\ \mathrm{s\,m^{-1}}$). Panel (a) shows a close-up of the box in panel (b). Again, the dashed and sinusoidal lines represent the P- and S-waves, respectively. The illustration highlights (1) some of the overburden interactions removed by the demultiple scheme (the black lines) and (2) the four strongest events remaining in the redatumed result (the red and blue lines). Event A is the desired target-related primary reflection, events B and D are forward-scattered waves, and event C (highlighted in blue) is a fast multiple. The dotted lines point to the arrivals associated with the illustrative arrows. For illustration purposes, all of the responses are convolved with a 30 Hz Ricker wavelet, and a global scaling factor is used to adjust the demultiple result to the reflection response.

by exploiting energy conservation and the minimum-phase property of the focusing function. The latter approach is discussed only conceptually and may enable the recovery of the focusing function $\mathbf{F}_1^+$, which will be discussed further in the future.

Remixed Marchenko demultiple method

The two Green's functions $\mathbf{G}^{-,\pm}$ are related by the redatumed reflection response $\mathbf{R}_{rd}$ (see equation 5) that is free of overburden interactions and, thus, is a form of overburden-borne multiple and forward-scattering elimination. In contrast, the remixed Green's functions $\mathbf{U}^{-,\pm}$ are mutually related by a target reflection response $\mathcal{R}$

$$\mathbf{U}^{-,+} = -\boldsymbol{\sigma}_z \mathbf{U}^{-,-}\mathcal{R}, \tag{25}$$

which can be retrieved using deconvolution (still per horizontal slowness s_x). By inserting an identity $\mathbf{B}^*(\mathbf{B}^*)^{-1}$ in equation 5, multiplying the result by $\mathbf{B}$ from the right, and using the definitions of the remixed Green's functions (see discussion of equation 14), we see that the target response $\mathcal{R}$ is related to the redatumed reflection response $\mathbf{R}_{rd}$ by

$$\mathcal{R} = (\mathbf{B}^*)^{-1}\mathbf{R}_{rd}^{\mathrm{T}}\boldsymbol{\sigma}_z\mathbf{B}. \tag{26}$$

In this process, we introduce a convolutional and matricial, more general, Moore-Penrose pseudoinverse of $\mathbf{B}$, denoted by the superscript "-1." Even though in our numerical experiments $\mathbf{B}$ is always invertible, we currently cannot offer any proof to assume invertibility in general. Moreover, for band-limited signals, the matrix inverse does not exist outside the spectral band of the signal, analogously to wavelet deconvolution. Unlike the Green's function $\mathbf{G}^{-,\pm}$, the remixed ones are easily calculable provided that the separability condition in equation 22 holds. The target reflection response $\mathcal{R}$ (see equation 26) is the desired redatumed reflection response, dressed with all overburden interactions described by $\mathbf{B}$ on the source and receiver sides. In a 1.5D acoustic case, $\mathbf{B}$ commutes with the redatumed reflection response $\mathbf{R}_{rd}$, and the product $(\mathbf{B}^*)^{-1}\mathbf{B}$ cancels except for a time shift defined by the overburden. However, in 2D, this is no longer the case. In the elastic situation, in the absence of fast multiples (see equation 12) $\mathbf{B}$ is an inverse time-reversed forward-scattered transmission through the overburden. This insight ties back to the statement in the "Introduction" section that forward-scattering cannot be predicted by existing methods. If equation 12 is violated, $\mathbf{B}$ also carries the imprint of fast multiples (e.g., see Figures 6 and 7 in Appendix D).

Moreover, the impact of forward scattering and fast multiples can be understood and tracked through the remixing operator (see equation 26). If the remixing operator can be retrieved, the aforementioned errors could even be corrected. This convenience is possible because the (remixed) Marchenko method only relies on linear scattering relations between fields defined in the overburden only and fields defined in the entire medium. In contrast, demultiple schemes that predict multiples only kinematically do not yet offer the opportunity to track the above-mentioned errors.

Alternative demultiple strategy

We conjecture that it could be possible to remove all of the overburden interactions, including forward scattering and (fast) multiples, by exploiting further physical constraints: energy conservation and the minimum-phase property of the focusing function. In the following, we make the first steps in this direction.

The up- and downgoing focusing functions conserve energy by

$$(\mathbf{F}_1^+)^\dagger\mathbf{F}_1^+ - (\mathbf{F}_1^-)^\dagger\mathbf{F}_1^- = \mathbf{I}; \tag{27}$$

that is, the net energy injected at z_0 equals the transmitted energy at z_i — a delta source at time zero. First, by evaluating energy conservation of the remixed focusing function, $\mathbf{V}_1^\pm = \mathbf{F}_1^\pm\mathbf{B}$, and using equation 27, we obtain the normal product of the remixing operator

$$(\mathbf{F}_1^+\mathbf{B})^\dagger\mathbf{F}_1^+\mathbf{B} - (\mathbf{F}_1^-\mathbf{B})^\dagger\mathbf{F}_1^-\mathbf{B} = \mathbf{B}^\dagger\mathbf{B}. \tag{28}$$

Second, we find a convolutional and matricial Moore-Penrose pseudoinverse of $\mathbf{B}^\dagger\mathbf{B}$, and we convolve the result by the remixed focusing function $\mathbf{V}_1^+$ from the left and right as

$$\mathbf{F}_1^+\mathbf{B}(\mathbf{B}^\dagger\mathbf{B})^{-1}(\mathbf{F}_1^+\mathbf{B})^\dagger = \mathbf{F}_1^+(\mathbf{F}_1^+)^\dagger. \tag{29}$$

The result is the normal product of the desired focusing function $\mathbf{F}_1^+$ and can be seen as a generalized power spectrum. Note that equations 27–29 also hold for band-limited wavefields. If the focusing function $\mathbf{F}_1^+$ can be retrieved from its normal product $\mathbf{F}_1^+(\mathbf{F}_1^+)^\dagger$, the desired Green's functions and hence the redatumed reflection response $\mathbf{R}_{rd}$, free of all overburden interactions, can be obtained (from equation 5).

We aim to retrieve the focusing function $\mathbf{F}_1^+$ from its normal product using a physical constraint. The focusing function $\mathbf{F}_1^+$ is an inverse of a transmission response. In 1D acoustics, this relation implies that the focusing function is a minimum-phase scalar function, except for a linear phase shift and hence possesses a unique amplitude-phase relationship through the Kolmogorov relation (Claerbout, 1985). This property allows Dukalski et al. (2019) and Elison et al. (2020) to factorize the (scalar) normal product $\mathbf{F}_1^+(\mathbf{F}_1^+)^\dagger$ and thereby predict short-period multiples that are generated in a horizontally layered acoustic overburden. In our case, the focusing function as a matrix is still an inverse transmission and therefore remains a minimum-phase object in a matrix sense. Tunnicliffe-Wilson (1972) proposes a method that factorizes the normal products of a subclass of minimum-phase matrices. The generalization of this method is the subject of ongoing research and will be published in the future. If this strategy can be successfully implemented, there is no need to retrieve the unknown operator $\mathbf{B}$. For an interested reader, however, we still present a numerical example of $\mathbf{B}$ in Appendix D.

NUMERICAL EXAMPLES

For horizontally layered media, all required wavefields can be modeled efficiently by wavefield extrapolation without band limitation (Kennett and Kerry, 1979; Hubral et al., 1980). Further, we choose the P- and S-wave velocities as well as the horizontal slownesses such that all events are on-sample; that is, the arrival times of all events are integer multiples of the temporal sampling interval (the medium parameters are specified in Appendix C). This allows us to better inspect the separability conditions of the conventional and remixed Marchenko methods because measurement-induced limitations are absent.

First, we consider the experiment in Figure 2a that satisfies the χ_--separability-condition of the conventional Marchenko method stated by equation 11. Using the correct initial estimate χ_+, which is obtained by applying the projector $\mathbf{P}^+$ (defined in Appendix B) to a modeled Green's function (i.e., the medium is known a priori), the elastodynamic Marchenko method finds the correct focusing function (see the trace in Figure 2a). However, when repeating this experiment for the model in Figure 2b, which violates the χ_--separability-condition in equation 11, the projector $\mathbf{P}^-$ erroneously preserves the first event of $\mathbf{G}^{-,+}$ (event II). Assuming that $\chi_- = \mathbf{O}$ forces this event to become part of the focusing function $\bar{\mathbf{F}}_1^-$ (the bar distinguishes retrieved from true solutions). To cancel multiples caused by this event, the retrieved $\bar{\mathbf{F}}_1^+$ contains an artifact (see the orange arrow in Figure 2b). Through the same mechanism, further artifacts are introduced.

Second, for the experiment shown in Figure 3a, which still satisfies the χ_--separability-condition in equation 11 as well as the χ_+-separability-condition in equation 12, the Marchenko series (see equation 10) finds the correct solution (see the trace in Figure 3a), using the forward-scattered part of the Green's function $(\mathbf{G}^{-,-})^*$ as the initial estimate. By downward shifting the second interface, as depicted in Figure 3b, equation 12 is violated and the overlap χ_+ is populated with fast multiples. If the initial estimate ignores these fast multiples, the Marchenko series does not converge to the true solution. For example, event IV, which is a (fast) multiple belonging to the Green's function, is now (erroneously) part of the focusing function (indicated by the orange-dotted line in Figure 3b). To compensate for these errors, the Marchenko series introduces further artifacts (in particular, see the errors after $t = -0.6$ s in Figure 3b).

Third, we repeat the previous experiment with the remixed Marchenko scheme, which simplifies the highly sophisticated initial estimate χ_+ to a trivial one $\chi_+^B = \mathbf{I}$. We use the remixed solutions to remove multiples according equation 26. Because there is only one reflector below the redatuming level, one would hope to eliminate all scattering effects except for a single primary (event A in Figure 6). Indeed, a significant amount of overburden interactions has been removed, revealing the primary A, which was masked by a strong multiple (see the traces and illustration in Figure 6). Nevertheless, the redatumed response still contains forward-scattered waves (e.g., events B and D) as well as fast multiples (e.g., event C). These remaining scattering effects are caused by remixing. The corresponding operator ($\mathbf{B}$) is angle dependent because it is implicitly defined by the overlap χ_+ (see the s_x-τ gathers shown in Figure 3; for an explicit example, see Appendix D). Following the alternative demultiple strategy that aims to remove all overburden interactions, we can already recover the normal product of the desired focusing function $\mathbf{F}_1^+$ near-perfectly (no figure), with a relative error below 1 ppm (for the model in Figures 3b and 6). Experiments on retrieving the focusing function from its normal product are beyond the scope of this paper.

CONCLUSION

Our analysis reveals that the conventional Marchenko method, similarly to the ISS, relies on a form of monotonicity, but in terms of one- instead of two-way traveltime. The former is a less restrictive condition. However, this advantage of the conventional Marchenko method must be compensated by providing an initial estimate, that is, prior information, which becomes challenging in practice. To remove the need for prior information, we introduce the remixed Marchenko scheme, which allows for a fair comparison with the requirements of the ISS. The remixed Marchenko scheme still relies on a less restrictive form of monotonicity than the ISS because it only requires the redatuming layer, instead of each layer in the overburden, to be sufficiently thick (in terms of the P-wave traveltime). Through this comparison, we gain significant insights about challenges of the elastic demultiple problem. We believe that these advances, and addressing the problems raised in this paper, are essential for further development of a full elastic Marchenko method.

Moreover, we present two strategies on how the remixed Marchenko equations can be used for multiple elimination. The first one can be easily implemented and removes all multiples that arrive after their generating primaries. The second strategy aims to remove all overburden-related effects, including forward scattering and (fast) multiples, by removing the remixing operator from the Marchenko solutions. For this purpose, additional physical constraints are taken into account, namely, energy conservation and the minimum-phase property of the (delayed) focusing function. The latter constraint is often associated with wavelets, but it is in fact a property of an entire wavefield, which we propose to exploit. Using a minimum-phase constraint for the prediction of forward-scattered waves and fast multiples requires minimum-phase matrix factorization, which is subject to ongoing research.

ACKNOWLEDGMENTS

This work was supported by the European Union's Horizon 2020 research and innovation program: Marie Skłodowska-Curie (grant no. 641943) and European Research Council (grant no. 742703). We would like to thank Kristopher Innanen and Dirk-Jan van Manen for reviewing and helping to improve this paper.

DATA AND MATERIALS AVAILABILITY

Data associated with this research are available and can be obtained by contacting the corresponding author.

APPENDIX A

DERIVATION OF THE REDATUMING RELATION

In this appendix, we derive the expression in equation 5 that relates the redatumed reflection response $\mathbf{R}_{rd}(s_x, z_i, \tau)$ to the retrieved Green's functions $\mathbf{G}^{-,\pm}(\pm s_x, z_0, z_i, \tau)$. For this derivation, we write all of the coordinates explicitly, but matrix products still imply temporal convolutions according to equation 4.

The starting point is the more familiar redatuming relation

$$\mathbf{G}^{-,+}(s_x, z_i, z_0, \tau) = \mathbf{R}_{rd}(s_x, z_i, \tau)\mathbf{G}^{+,+}(s_x, z_i, z_0, \tau). \quad \text{(A-1)}$$

Next, we use source-receiver reciprocity (Wapenaar, 2014)

$$\mathbf{G}^{\mp,+}(s_x, z_i, z_0, \tau) = \pm[\mathbf{G}^{-,\pm}(-s_x, z_0, z_i, \tau)]^{\mathrm{T}}, \quad \text{(A-2)}$$

and to interchange source and receiver in equation A-1

$$\begin{aligned}\mathbf{G}^{-,+}(s_x, z_0, z_i, \tau) &= [\mathbf{G}^{-,+}(-s_x, z_i, z_0, \tau)]^{\mathrm{T}},\\ &= [\mathbf{G}^{+,+}(-s_x, z_i, z_0, \tau)]^{\mathrm{T}}[\mathbf{R}_{rd}(-s_x, z_i, \tau)]^{\mathrm{T}},\\ &= -\mathbf{G}^{-,-}(s_x, z_0, z_i, \tau)[\mathbf{R}_{rd}(-s_x, z_i, \tau)]^{\mathrm{T}}. \end{aligned} \tag{A-3}$$

In horizontally layered media, wavefields associated with positive and negative horizontal slownesses s_x are mutually related through multiplication by a Pauli matrix $\boldsymbol{\sigma}_z$ (multiplied by a temporal delta spike) from the left and right, which yields

$$\begin{aligned}&\mathbf{G}^{-,+}(s_x, z_0, z_i, \tau)\\ &= -\boldsymbol{\sigma}_z\mathbf{G}^{-,-}(-s_x, z_0, z_i, \tau)\boldsymbol{\sigma}_z\boldsymbol{\sigma}_z[\mathbf{R}_{rd}(s_x, z_i, \tau)]^{\mathrm{T}}\boldsymbol{\sigma}_z,\\ &= -\boldsymbol{\sigma}_z\mathbf{G}^{-,-}(-s_x, z_0, z_i, \tau)[\mathbf{R}_{rd}(s_x, z_i, \tau)]^{\mathrm{T}}\boldsymbol{\sigma}_z. \end{aligned} \tag{A-4}$$

APPENDIX B

DERIVATION OF SEPARABILITY CONDITIONS

In this appendix, we formulate the separability conditions of the ISS and of the original as well as the remixed representation theorems. Furthermore, we derive explicit expression of the projectors $\mathbf{P}^{\pm}$ and $\mathbf{P}^{\pm}_{B}$.

Consider a homogeneous layer (labeled by k) of thickness $\Delta z^{(k)}$ as well as P- and S-wave velocities $c^{(k)}_{\mathrm{P}}$ and $c^{(k)}_{\mathrm{S}}$. For a plane wave with horizontal slowness s_x, P- and S-waves propagate with the vertical slowness

$$s^{(k)}_{z,\mathrm{P/S}} = \sqrt{(c^{(k)}_{\mathrm{P/S}})^{-2} - s_x^2}. \tag{B-1}$$

The resulting one-way traveltime of such a plane wave through layer k is

$$\tau^{(k)}_{\mathrm{P/S}} = \Delta z^{(k)} s^{(k)}_{z,\mathrm{P/S}}. \tag{B-2}$$

In the following, we assume that the P-wave velocity

$$c_{\mathrm{P}} = \sqrt{\frac{\lambda + 2\mu}{\rho}} \tag{B-3}$$

is greater than the S-wave velocity

$$c_{\mathrm{S}} = \sqrt{\frac{\mu}{\rho}} \tag{B-4}$$

de Hoop (1995), which is the case for most materials: the shear modulus μ and the density ρ are always positive. The first Lamé parameter λ can be negative, but for all natural materials known to the authors the relation $\lambda > -\mu$ holds.

Separability of conventional representation theorems

In the following, we derive the separability conditions implied by the conventional Marchenko scheme.

First, we analyze the separability of the focusing function $\mathbf{F}^{-}_{1}$ from the Green's function $\mathbf{G}^{-,+}$ on the left side of equation 6. To guarantee separability, the last and first events of the focusing and Green's functions must satisfy the condition

$$\tau_{\Omega}(F^{-}_{1,ab}) < \tau_{\alpha}(G^{-,+}_{ab}), \tag{B-5}$$

for each elastic component combination ab. Here, the functions τ_{α} and τ_{Ω} denote the first and last arrival times at the recording level z_0, respectively. We sum the one-way traveltimes along the travel path of the last event of $F^{-}_{1,ab}$ (e.g., for $F^{-}_{1,\mathrm{SP}}$, see event I in Figure 2a, and see Figure 5 for layer labeling $i_{0/1}$)

$$\tau_{\Omega}(F^{-}_{1,ab}) = \tau^{(0)}_{a} + \sum_{k=1}^{i-1}\tau^{(k)}_{\mathrm{S}} - \tau^{(i_0)}_{b}, \tag{B-6}$$

and along the travel path of the first event of $G^{-,+}_{ab}$ (e.g., for $G^{-,+}_{\mathrm{SP}}$ see event II in Figure 2a),

$$\tau_{\alpha}(G^{-,+}_{ab}) = \tau^{(0)}_{a} + \sum_{k=1}^{i}\tau^{(k)}_{\mathrm{P}} + \tau^{(i_1)}_{b}. \tag{B-7}$$

We substitute equations B-6 and B-7 in equation B-5, replace the one-way traveltimes by equation B-2, and obtain the χ_{-}-separability-condition of equation 11

$$\sum_{k=1}^{i-1}\Delta z^{(k)}(s^{(k)}_{z,\mathrm{S}} - s^{(k)}_{z,\mathrm{P}}) < 2\Delta z^{(i)} s^{(i)}_{z,\mathrm{P}}. \tag{B-8}$$

Second, we derive a condition under which the overlap χ_{+} simplifies to the forward-scattered part of the Green's function $(\mathbf{G}^{-,-})^{*}$. This scenario requires that the fastest multiple coda of the (time reversed) Green's function $(\mathbf{G}^{-,-})^{*}$ reaches the recording level before the first event of the focusing function $\mathbf{F}^{+}_{1}$ (which defines the first event of the overlap χ_{+})

$$\tau_{\Omega}[(G^{-,-}_{m,ab})^{*}] < \tau_{\alpha}(F^{+}_{1,ab}). \tag{B-9}$$

Here, we use subscript m to refer to the multiples of a wavefield. We sum the one-way traveltimes along the path of the fastest multiple coda of the Green's function $(G^{-,-}_{m,ab})^{*}$ (e.g., for $(G^{-,-}_{m,\mathrm{SP}})^{*}$, see event IV in Figure 3a) by

$$\tau_{\Omega}[(G^{-,-}_{m,ab})^{*}] = -\tau^{(0)}_{a} - \sum_{k=1}^{i-1}\tau^{(k)}_{\mathrm{P}} - 2\min\{\tau^{(k)}_{\mathrm{P}} | k \in [1,i]\} - \tau^{(i_0)}_{b}, \tag{B-10}$$

and along the travel path of the first event of the focusing function $F^{+}_{1,ab}$ (e.g., for $F^{+}_{1,\mathrm{SP}}$, see event III in Figure 3a)

$$\tau_{\alpha}(F^{+}_{1,ab}) = -\tau^{(0)}_{a} - \sum_{k=1}^{i-1}\tau^{(k)}_{\mathrm{S}} - \tau^{(i_0)}_{b}. \tag{B-11}$$

We substitute equations B-10 and B-11 in equation B-9, express the one-way traveltimes according to equation B-2, and arrive at the χ_{+}-separability-condition

$$\sum_{k=1}^{i-1}\Delta z^{(k)}(s^{(k)}_{z,\mathrm{S}} - s^{(k)}_{z,\mathrm{P}}) < 2\,\min\{\Delta z^{(k)} s^{(k)}_{z,\mathrm{P}} | k \in [1,i]\}. \tag{B-12}$$

This condition can only be satisfied if the separability condition in equation B-8 holds.

If the separability condition in equation B-8 holds, the projector $\mathbf{P}^{-}$, acting as a Hadamard matrix product in the P-S space, separates the convolution-type representation theorem in equation 6 according to

$$\mathbf{P}^{-}[\mathbf{G}^{-,+}] = \boldsymbol{\chi}_{-} = \mathbf{O}, \tag{B-13}$$

$$\mathbf{P}^{-}[\mathbf{F}_{1}^{-}] = \mathbf{F}_{1}^{-}. \tag{B-14}$$

We define the projector $\mathbf{P}^{-}$, such that all events after the last arrival of the focusing function $\mathbf{F}_{1}^{-}$ are muted,

$$P_{ab}^{-} = \mathrm{H}[-\tau + \tau_{\Omega}(F_{1,ab}^{-})] = \mathrm{H}(-\tau + \tau_{a}^{(0)} + \sum_{k=1}^{i-1} \tau_{\mathrm{S}}^{(k)} - \tau_{b}^{(i_0)}), \tag{B-15}$$

where we use equation B-6. The function $\mathrm{H}(\tau)$ denotes the Heaviside function, $\mathrm{H}(\tau < 0) = 0$ and $\mathrm{H}(\tau \geq 0) = 1$. In analogy, the correlation-type representation theorem in equation 7 can be separated with a projector $\mathbf{P}^{+}$ as

$$\mathbf{P}^{+}[(\mathbf{G}^{-,-})^{*}] = \boldsymbol{\chi}_{+}, \tag{B-16}$$

$$\mathbf{P}^{+}[\mathbf{F}_{1}^{+}] = \mathbf{F}_{1}^{+}, \tag{B-17}$$

that mutes all events before the first arrival of the focusing function $\mathbf{F}_{1}^{+}$,

$$P_{ab}^{+} = \mathrm{H}[\tau - \tau_{\alpha}(F_{1,ab}^{+})] = \mathrm{H}(\tau + \tau_{a}^{(0)} + \sum_{k=1}^{i-1} \tau_{\mathrm{S}}^{(k)} + \tau_{b}^{(i_0)}). \tag{B-18}$$

In the latter expression, we use equation B-11.

Separability of remixed representation theorems

In the section, "Marchenko method with trivial initial estimate," we introduce an unknown operator $\mathbf{B}$ to transform the overlap $\boldsymbol{\chi}_{+}$ between the focusing function $\mathbf{F}_{1}^{+}$ and the Green's function $(\mathbf{G}^{-,-})^{*}$ to a trivial one. Thus, the remixed correlation-type representation theorem in equation 14 is separable by definition, except for an identity matrix. However, the separability of the remixed convolution-type representation theorem in equation 13 is not guaranteed and is assessed below.

The remixed representation theorem in equation 13 is separable if the last event of the remixed focusing function $\mathbf{V}_{1}^{-}$ arrives at the recording surface before the first event of the remixed Green's function $\mathbf{U}^{-,+}$

$$\tau_{\Omega}(V_{1,ab}^{-}) < \tau_{\alpha}(U_{ab}^{-,+}), \tag{B-19}$$

which can be rewritten as

$$\tau_{\Omega}(F_{1,a\mathrm{S}}^{-}) + \tau_{\Omega}(B_{\mathrm{S}b}) < \tau_{\alpha}(G_{a\mathrm{P}}^{-,+}) + \tau_{\alpha}(B_{\mathrm{P}b}). \tag{B-20}$$

Now, we define the first and last arrival times of the remixing operator $\mathbf{B}$. The remixing operator projects the Green's function $(\mathbf{G}^{-,-})^{*}$ onto an identity matrix plus an acausal coda. Hence, the first event of the remixing operator coincides with the first event of the inverse $((\mathbf{G}^{-,-})^{*})^{-1}$. For example, the first, but time reversed, event of B_{PS} is depicted by path V in Figure 3b. We sum the one-way traveltimes along this path for an arbitrary component ab by

$$\tau_{\alpha}(B_{ab}) = \tau_{a}^{(i_0)} + \sum_{k=1}^{i-1} \tau_{\mathrm{P}}^{(k)} + \tau_{b}^{(0)}. \tag{B-21}$$

Further, we heuristically assume that the remixing operator has the same temporal extent as the overlap $\boldsymbol{\chi}_{+}$ between the focusing function $\mathbf{F}_{1}^{+}$ and the Green's function $(\mathbf{G}^{-,-})^{*}$, which is $\sum_{k=1}^{i-1}(\tau_{\mathrm{S}}^{(k)} - \tau_{\mathrm{P}}^{(k)})$. As a result, the one-way traveltime of the last event of the remixing operator is

$$\tau_{\Omega}(B_{ab}) = \tau_{a}^{(i_0)} + \sum_{k=1}^{i-1} \tau_{\mathrm{S}}^{(k)} + \tau_{b}^{(0)}. \tag{B-22}$$

Thorough empirical investigations confirm this result. Upon substituting equations B-6 and B-7 and equations B-21 and B-22 in equation B-20 and using equation B-2, we find the $\boldsymbol{\chi}_{-}^{B}$-separability-condition for the remixed Marchenko scheme

$$\sum_{k=1}^{i-1} \Delta z^{(k)}(s_{z,\mathrm{S}}^{(k)} - s_{z,\mathrm{P}}^{(k)}) < \Delta z^{(i)} s_{z,\mathrm{P}}^{(i)}. \tag{B-23}$$

Note that the choice of level z_i within the ith layer (labeling $i_{0/1}$) is used for the derivation but is dropped in the separability conditions in equations B-8, B-12, and B-23.

Now, we derive expressions for the remixed projectors $\mathbf{P}_{B}^{\pm}$. Analogous to the derivation of the separability conditions, we use arrival times of first and last events of specific wavefields to find the remixed projectors. From equations 15 and 16, it follows that the remixing operator $\mathbf{B}$ unfolds the overlap $\boldsymbol{\chi}_{+}$ between focusing function $\mathbf{F}_{1}^{+}$ and Green's function $(\mathbf{G}^{-,-})^{*}$, except for an identity matrix. As a consequence, the diagonal elements of the projector $\mathbf{P}_{B}^{+}$ should only preserve positive times, including time zero to account for equation 15, such that

$$P_{B,\mathrm{PP}}^{+} = P_{B,\mathrm{SS}}^{+} = \mathrm{H}(\tau). \tag{B-24}$$

The first arrival times of the individual matrix elements $V_{ab}^{+} = F_{1,ac}^{+} B_{cb}$ only differ by an a-wave propagation of $F_{1,ac}^{+}$ and a b-wave propagation of B_{cb}, through the top layer. Hence, the diagonal elements of the projector $\mathbf{P}_{B}^{+}$ in equation B-24 can be generalized to an arbitrary projector element

$$P_{B,ab}^{+} = \mathrm{H}[\tau + (1 - \delta_{ab})\Delta z^{(0)}(s_{z,a}^{(0)} - s_{z,b}^{(0)})], \tag{B-25}$$

where δ_{ab} denotes the Kronecker delta.

Next, we derive an expression for the projector $\mathbf{P}_{B}^{-}$. The remixing operator is not designed to modify the focusing function $\mathbf{F}_{1}^{-}$ or the Green's function $\mathbf{G}^{-,+}$ in a special way. Therefore, in a general case, the arrival time of the last event of the remixed focusing function $V_{ab}^{-} = F_{1,ac}^{-} B_{cb}$ is obtained by adding the last arrival times of the focusing function $F_{1,a\mathrm{S}}^{-}$ and the remixing operator $B_{\mathrm{S}b}$:

$$P^-_{B,ab} = \mathrm{H}(\tau - [\tau_\Omega(F^-_{1,a\mathrm{S}}) + \tau_\Omega(B_{\mathrm{S}b})]),$$
$$= \mathrm{H}[\tau - \Delta z^{(0)}(s^{(0)}_{z,a} + s^{(0)}_{z,b}) - 2\sum_{k=1}^{i-1}\Delta z^{(k)} s^{(k)}_{z,\mathrm{S}}], \quad \text{(B-26)}$$

where we use equations B-2, B-6, and B-22.

Although the expressions for the remixed projectors might appear complicated, they can be constructed easily from (1) a smooth P- and S-wave velocity model combined with (2) an estimate of the position of the shallowest reflector and (3) an estimate of the position of the reflector above the redatuming depth. The latter estimate could be obtained, for example, by selecting a redatuming depth below a strong reflector that can be easily localized. Compared to the conventional elastodynamic Marchenko method, the required a priori knowledge is significantly reduced.

From monotonicity to separability conditions

In this appendix, we quantify the monotonicity assumptions of the ISS as separability conditions.

The monotonicity assumption (1) requires temporal ordering of primaries according to the reflector ordering in depth. Hence, for an arbitrary elastic component of the reflection response R_{ab}, the slowest primary associated with an interface $j-1$ (at the bottom of layer $j-1$) must reach the recording surface before the fastest primary associated with the next, deeper, interface j (see Figure 5):

$$\tau_\Omega(R^{(j-1)}_{ab}) < \tau_\alpha(R^{(j)}_{ab}). \quad \text{(B-27)}$$

The superscripts refer to (converted) primary reflections associated with interfaces $j-1$ and j. Now, we sum the traveltimes along the travel path of these two primaries, leading to

$$\tau_\Omega(R^{(j-1)}_{ab}) = \tau^{(0)}_a + 2\sum_{k=1}^{j-1}\tau^{(k)}_{\mathrm{S}} + \tau^{(0)}_b, \quad \text{(B-28)}$$

and

$$\tau_\alpha(R^{(j)}_{ab}) = \tau^{(0)}_a + 2\sum_{k=1}^{j}\tau^{(k)}_{\mathrm{P}} + \tau^{(0)}_b. \quad \text{(B-29)}$$

Next, we substitute equations B-28 and B-29 in equation B-27, replace the traveltimes by equation B-2, and obtain a separability condition

$$\sum_{k=1}^{j-1}\Delta z^{(k)}(s^{(k)}_{z,\mathrm{S}} - s^{(k)}_{z,\mathrm{P}}) < \Delta z^{(j)} s^{(j)}_{z,\mathrm{P}}. \quad \text{(B-30)}$$

Redatuming from the recording level z_0 to z_i requires that all of the interfaces between these two depth levels satisfy monotonicity; that is, equation B-30 becomes the separability condition in equation 23.

The monotonicity assumption (2) requires that multiples are recorded after their generating primaries. Hence, for redatuming to the depth level z_i the slowest primary reflection associated with the interface $i-1$ must predate the fastest multiple generated by the same interface

$$\tau_\Omega(R^{(i-1)}_{ab}) < \tau_\alpha(R^{(i-1)}_{m,ab}), \quad \text{(B-31)}$$

where $R^{(i-1)}_{m,ab}$ represents the multiples generated by the interface $i-1$. Again, we sum the traveltimes along the paths of these two events

$$\tau_\Omega(R^{(i-1)}_{ab}) = \tau^{(0)}_a + 2\sum_{k=1}^{i-1}\tau^{(k)}_{\mathrm{S}} + \tau^{(0)}_b \quad \text{(B-32)}$$

and

$$\tau_\alpha(R^{(i-1)}_{m,ab}) = \tau^{(0)}_a + 2\sum_{k=1}^{i-1}\tau^{(k)}_{\mathrm{P}} + 2\,\min\{\tau^{(k)}_{\mathrm{P}}|k\in[1,i]\} + \tau^{(0)}_b. \quad \text{(B-33)}$$

Upon substituting equations B-32 and B-33 in equation B-31 and replacing the traveltimes by equation B-2, the monotonicity assumption (2) can be written as

$$\sum_{k=1}^{i-1}\Delta z^{(k)}(s^{(k)}_{z,\mathrm{S}} - s^{(k)}_{z,\mathrm{P}}) < \min\{\Delta z^{(k)} s^{(k)}_{z,\mathrm{P}}|k\in[1,i]\}, \quad \text{(B-34)}$$

which is the separability condition in equation 24. Note that, for multiple generators above the interface $i-1$, the condition in equation B-34 is relaxed because the left side will remain constant or decrease, whereas the right side will remain constant or increase.

Table C-1. The medium parameters used for the experiment shown in Figures 1 and 2a (for the acoustic experiment, the S-wave velocity is set to zero). The focusing depth is at $z_f = 1902.07$ m. The experiment shown in Figure 2b uses the same medium parameters, except that the bottom interface is moved from $z = 2501.07$ to $z = 2299.00$ m.

z(m)	$c_{\mathrm{P}}(\mathrm{m\,s^{-1}})$	$c_{\mathrm{S}}(\mathrm{m\,s^{-1}})$	$\rho(\mathrm{kg\,m^{-3}})$
−∞–500	1993.63	898.38	4200
500–1700	1897.78	1099.20	1100
1700–2501.07	2500.00	1386.75	6000
2501.07–∞	2695.26	1611.32	3500

Table C-2. The medium parameters used for the experiment shown in Figure 3a. The focusing depth is at $z_f = 1703.42$ m. The experiment shown in Figure 3b uses the same medium parameters, except that the second interface from above is moved from $z = 1250.56$ to $z = 1452.63$ m.

z(m)	$c_{\mathrm{P}}(\mathrm{m\,s^{-1}})$	$c_{\mathrm{S}}(\mathrm{m\,s^{-1}})$	$\rho(\mathrm{kg\,m^{-3}})$
−∞–500	1993.63	898.38	1100
500–1250.56	2500	1796.05	4200
1250.56–1503.15	1505.43	1050.85	1700
1503.15–2304.24	1900.00	1006.04	6000
2304.24–∞	2695.26	1396.65	3500

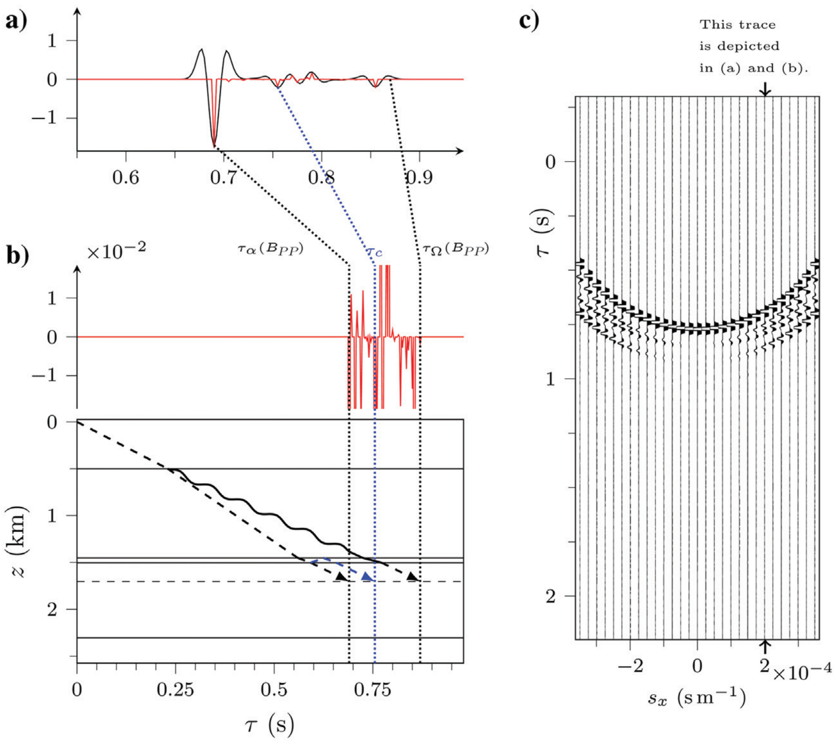

Figure D-1. Remixing operator **B** associated with the numerical example in Figure 6 (arbitrarily chosen PP component). Panel (a) shows the remixing operator before (red) and after (black) convolution with a 30 Hz Ricker wavelet. In panel (b), the clipping values of the time and amplitude axes are adjusted to highlight the travel paths associated with three selected events of the remixing operator: (1) the first event of B_{PP}, (2) a fast multiple that persists in the demultiple result (see event C in Figure 6), and (3) the last event of B_{PP}. Due to its small amplitude, the last event is only visible in panel (b). The dotted lines point to the arrivals associated with the illustrative arrows and label the traveltimes of these events as $\tau_\alpha(B_{\mathrm{PP}})$, τ_c, and $\tau_\Omega(B_{\mathrm{PP}})$. Again, the dashed and sinusoidal lines represent the P- and S-waves, respectively. Panel (c) shows an s_x-τ gather of the remixing operator (after convolution with a 30 Hz Ricker wavelet). By analyzing all of the elastic components (not shown here), it can be seen that operator **B** is a scaled and delayed identity plus a small coda. Hence, its determinant is approximately a phase shift with a nonzero amplitude, meaning that **B** is invertible.

APPENDIX C

MEDIUM PARAMETERS

This appendix contains the medium parameters used for the experiments shown in Figures 1–3 (see Tables C-1 and C-2). Note that the values of the medium parameters are adjusted to ensure all events associated with the horizontal slowness $s_x = 2 \times 10^{-4}$ m are recorded on-sample; that is, the traveltime of each event is an integer multiple of the temporal sampling interval. The values are within a reasonable range but are not associated with any specific material. We use exaggerated density contrasts to generate strong, well-visible events. In realistic media, the contrasts may be weaker but are much more numerous. Hence, there will be many weak, as opposed to a few strong, converted waves. The Marchenko method and the separability conditions are independent of the number and strength of these events; thus, our analysis also holds in more realistic media.

APPENDIX D

NUMERICAL EXAMPLE OF THE REMIXING OPERATOR

In this appendix, we determine and show the remixing operator associated with the experiment in Figure 6. Because, to our knowledge, operator **B** cannot be computed directly, we obtain it indirectly. First, we retrieve $\mathbf{V}_1^\pm$ by solving the remixed representation theorems (provided that the χ_-^B-separability-condition in equation 22 holds) and model $\mathbf{F}_1^\pm$ through wavefield extrapolation. Second, we obtain the remixing operator **B** by solving

$$\mathbf{V}_1^\pm = \mathbf{F}_1^\pm \mathbf{B} \tag{D-1}$$

by deconvolution. We carry out this deconvolution for up- and downgoing fields independently to confirm that both cases lead to the same solution. The resulting remixing operator (see Figure D-1) has a finite duration of

$$\tau_\Omega(B_{\mathrm{PP}}) - \tau_\alpha(B_{\mathrm{PP}}) = 0.18 \text{ s}, \tag{D-2}$$

which is equal to the expected one (using equations B-2, B-21, and B-22) of

$$\tau_\Omega(B_{\mathrm{PP}}) - \tau_\alpha(B_{\mathrm{PP}}) = \sum_{k=1}^{i-1} \Delta z^{(k)} (s_{z,\mathrm{S}}^{(k)} - s_{z,\mathrm{P}}^{(k)}). \tag{D-3}$$

Moreover, the remixing operator contains a fast multiple at $\tau = \tau_c$, which constructs event C in Figure 6 via equation 26. At zero incidence, the remixing operator simplifies to a single event (see the s_x-τ gather in Figure D-1c).

REFERENCES

Amundsen, L., 2001, Elimination of free-surface related multiples without need of the source wavelet: Geophysics, **66**, 327–341, doi: 10.1190/1.1444912.

Bava, G. P., and G. Ghione, 1984, Inverse scattering for optical couplers. Exact solution of Marchenko equations: Journal of Mathematical Physics, 1904–1900 ,**25**, doi: 10.1063/1.526379.

Broggini, F., R. Snieder, and K. Wapenaar, 2012, Focusing the wavefield inside an unknown 1D medium: Beyond seismic interferometry: Geophysics, **77**, no. 5, A25–A28, doi: 10.1190/geo2012-0060.1.

Claerbout, J. F., 1985, Imaging the earth's interior: Blackwell Scientific Publications Oxford.

Coates, R. T., and A. B. Weglein, 1996, Internal multiple attenuation using inverse scattering: Results from prestack 1 & 2D acoustic and elastic synthetics: 66th Annual International Meeting, SEG, Expanded Abstracts, 1522–1525, doi: 10.1190/1.1826408.

de Hoop, A. T., 1995, Handbook of radiation and scattering of waves: Acoustic waves in fluids, elastic waves in solids, electromagnetic waves: Academic Press.

Dukalski, M., and K. de Vos, 2017, Marchenko inversion in a strong scattering regime including surface-related multiples: Geophysical Journal International, **212**, 760–776, doi: 10.1093/gji/ggx434.

Dukalski, M., and K. de Vos, 2020, A closed formula for true-amplitude overburden-generated interbed de-multiple: 82nd Annual International Conference and Exhibition, EAGE, Extended Abstracts.

Dukalski, M., E. Mariani, and K. de Vos, 2019, Handling short-period scattering using augmented Marchenko autofocusing: Geophysical Journal International, **216**, 2129–2133, doi: 10.1093/gji/ggy544.

El-Emam, A., A. Mohamed, and H. Al-Qallaf, 2001, Multiple attenuation techniques, case studies from Kuwait: 71st Annual International Meeting, SEG, Expanded Abstracts, 1317–1320, doi: 10.1190/1.1816339.

Elison, P., M. Dukalski, K. de Vos, D. van Manen, and J. Robertsson, 2020, Data-driven control over short-period internal multiples in media with a horizontally layered overburden: Geophysical Journal International, **221**, 769–787, doi: 10.1093/gji/ggaa020.

Frasier, C. W., 1970, Discrete time solution of plane P-SV waves in a plane layered medium: Geophysics, **35**, 197–219, doi: 10.1190/1.1440085.

Hubral, P., S. Treitel, and P. R. Gutowski, 1980, A sum autoregressive formula for the reflection response: Geophysics, **45**, 1697–1705, doi: 10.1190/1.1441061.

Jakubowicz, H., 1998, Wave equation prediction and removal of interbed multiples: 68th Annual International Meeting, SEG, Expanded Abstracts, 1527–1530, doi: 10.1190/1.1820204.

Kennett, B. L. N., and N. J. Kerry, 1979, Seismic waves in a stratified half-space: Geophysical Journal International, **57**, 557–583, doi: 10.1111/j.1365-246X.1979.tb06779.x.

Meles, G. A., K. Wapenaar, and J. Thorbecke, 2018, Virtual plane-wave imaging via Marchenko redatuming: Geophysical Journal International, **214**, 508–519, doi: 10.1093/gji/ggy143.

Mildner, C., M. Dukalski, P. Elison, K. D. Vos, F. Broggini, and J. O. A. Robertsson, 2019, True amplitude-versus-offset Green's function retrieval using augmented Marchenko focusing: 81st Annual International Conference and Exhibition, EAGE, Extended Abstracts, 1–5, doi: 10.3997/2214-4609.201900839.

Nita, B. G., and A. B. Weglein, 2009, Pseudo-depth/intercept-time monotonicity requirements in the inverse scattering algorithm for predicting internal multiple reflections: Communications in Computational Physics, **5**, 163.

Ravasi, M., I. Vasconcelos, A. Kritski, A. Curtis, C. A. da Costa Filho, and G. A. Meles, 2016, Target-oriented Marchenko imaging of a North Sea field: Geophysical Journal International, **205**, 99–104, doi: 10.1093/gji/ggv528.

Reinicke, C., M. Dukalski, and K. Wapenaar, 2019, Do we need elastic internal de-multiple offshore Middle East, or will acoustic Marchenko suffice: Presented at the SEG/KOC Workshop: Seismic Multiples — The Challenges and the Way Forward, Kuwait.

Reinicke, C., G. A. Meles, and K. Wapenaar, 2018, Elastodynamic plane wave Marchenko redatuming: Theory and examples: 80th Annual International Conference and Exhibition, EAGE, Extended Abstracts, 1–5, doi: 10.3997/2214-4609.201801341.

Slob, E., K. Wapenaar, F. Broggini, and R. Snieder, 2014, Seismic reflector imaging using internal multiples with Marchenko-type equations: Geophysics, **79**, no. 2, S63–S76, doi: 10.1190/geo2013-0095.1.

Staring, M., R. Pereira, H. Douma, J. van der Neut, and K. Wapenaar, 2018, Source-receiver Marchenko redatuming on field data using an adaptive double-focusing method: Geophysics, **83**, no. 6, S579–S590, doi: 10.1190/geo2017-0796.1.

Sun, J., and K. A. Innanen, 2016, Interbed multiple prediction on land: Which technology, and which domain? Recorder, **41**, 24–29.

Sun, J., and K. A. Innanen, 2019, A plane-wave formulation and numerical analysis of elastic multicomponent inverse scattering series internal multiple prediction: Geophysics, **84**, no. 5, V255–V269, doi: 10.1190/geo2018-0259.1.

Tunnicliffe-Wilson, G., 1972, The factorization of matricial spectral densities: SIAM Journal on Applied Mathematics, **23**, 420–426, doi: 10.1137/0123044.

Ursin, B., 1983, Review of elastic and electromagnetic wave propagation in horizontally layered media: Geophysics, **48**, 1063–1081, doi: 10.1190/1.1441529.

van der Neut, J., and K. Wapenaar, 2016, Adaptive overburden elimination with the multidimensional Marchenko equation: Geophysics, **81**, no. 5, T265–T284, doi: 10.1190/geo2016-0024.1.

Wapenaar, K., 2014, Single-sided Marchenko focusing of compressional and shear waves: Physical Review E, **90**, 63202, doi: 10.1103/PhysRevE.90.063202.

Wapenaar, K., F. Broggini, E. Slob, and R. Snieder, 2013, Three-dimensional single-sided Marchenko inverse scattering, data-driven focusing, Green's function retrieval, and their mutual relations: Physical Review Letters, **110**, 084301, doi: 10.1103/PhysRevLett.110.084301.

Wapenaar, K., and E. Slob, 2015, Initial conditions for elastodynamic Green's function retrieval by the Marchenko method: 85th Annual International Meeting, SEG, Expanded Abstracts, 5074–5080, doi: 10.1190/segam2015-5916768.1.

Wapenaar, K., J. Thorbecke, J. van der Neut, F. Broggini, E. Slob, and R. Snieder, 2014, Marchenko imaging: Geophysics, **79**, no. 3, WA39–WA57, doi: 10.1190/geo2013-0302.1.

Ware, J. A., and K. Aki, 1969, Continuous and discrete inverse-scattering problems in a stratified elastic medium — 1: Plane waves at normal incidence: The Journal of the Acoustical Society of America, **45**, 911–921, doi: 10.1121/1.1911568.

Weglein, A. B., F. A. Gasparotto, P. M. Carvalho, and R. H. Stott, 1997, An inverse-scattering series method for attenuating multiples in seismic reflection data: Geophysics, **62**, 1975–1989, doi: 10.1190/1.1444298.

Zakharov, V. E., and A. B. Shabat, 1973, Interaction between solitons in a stable medium: Soviet Physics JETP, **37**, 823–828.